

# Road Surface Crack Detection: Improved Segmentation with Pixel-based Refinement

Henrique Oliveira

Instituto de Telecomunicações, Lisbon  
Instituto Politécnico de Beja  
Portugal  
hjmo@lx.it.pt

Paulo Lobato Correia

Instituto de Telecomunicações – Instituto Superior Técnico  
Lisbon, Portugal  
plc@lx.it.pt

**Abstract**— Cracks are among the most commonly found road surface degradations, requiring periodical road surveys for monitoring pavement quality. Images of road pavement surface can be automatically processed, typically employing segmentation algorithms to identify cracks. However, a set of distinct connected components often result, leading to the detection of several independent crack segments, although they may belong to the same pavement surface defect. This is often observed for cracks that exhibit a longer linear development or present several branches. This paper presents a new strategy to identify cracks on images captured during road pavement surveys, even when those cracks appear with a complex shape. The proposed crack segmentation algorithm includes two stages: (i) selection of prominent “crack seeds”, adopting an efficient segmentation procedure, after appropriate image smoothing, minimizing the detection of false positives; (ii) iterative binary pixel classification, into the crack or non-crack classes, extending the “seeds” to identify the complete crack shape. The paper also tests the combination of the proposed two stage crack segmentation with three smoothing techniques, to evaluate their suitability for crack detection. As a final step the system classifies the identified cracks as longitudinal, transversal or miscellaneous types. Tests performed with images acquired from different types of sensors (active and non-active), show improved crack segmentation results.

**Keywords**—Crack detection; Road surface; Segmentation; Pattern Recognition; Image Processing

## I. INTRODUCTION

Periodic road pavement surveys are among the most important tools used to collect data for planning and scheduling maintenance and repair actions. Cracks are the most common defects found on images acquired during such surveys. Cracking appears in pavement surfaces mainly due to fatigue of the asphaltic (top) pavement layers, but also caused by adverse atmospheric conditions, that may cause shrinkage of materials, or to construction problems motivated by a bad quality of the asphaltic mixtures or by weaknesses in the structural pavement resistance. Technicians and engineers dealing with road surface maintenance do not share a single definition of what a crack means. Its definition can be slightly different in different countries, or when working with different pavement types. One relevant definition was proposed by the American Association of State Highway and Transportation Officials (AASHTO) [1]: “A crack is a discontinuity in the pavement surface with minimum dimensions of 1 mm width and 25 mm length”. Other definitions refer the expected geometric characteristics of cracks, although not providing

quantification information. For instance, the definition by the World Road Association [2] is: “A crack is a discontinuity in the road surface that has a minimum length, width and depth”.

For the purpose of this paper, it is important to recall that in early development stages, small cracks may appear isolated, or as a series of interconnected components, while in later stages they appear connected and with a higher density pattern. Therefore, this paper proposes that the definition of a crack encompasses its lifecycle, being an observable discontinuity in the road surface, whose width and length are sufficient to distinguish it from spurious non-uniformities of the top layer or stains in the pavement, caused by oil or other materials, and that if several such discontinuities are close together and present a similar aspect and orientation, then they should be considered as belonging to the same crack.

One of the most challenging tasks when applying automatic crack detection and characterization systems is the identification of narrow and short sections of cracks, especially in cases where these cracks exhibit highly variable shapes, for instance including several crack branches of highly variable widths along their development. Minimal path based methods, Markovian modelling with geometric constraints and Free Form Anisotropy algorithms have been used to solve the detection of cracks with a complex shape [3]. Short discontinuities in cracks occur often, so automatic detection algorithms should decide whether to label them as independent cracks, or as belonging to the same pavement crack, linking them together.

This paper proposes a novel crack segmentation algorithm, based on a set of iterative statistical tests, able to link together narrow and short sections of cracks that are typically identified as separate connected components. After an identification of cracks seeds, by applying an efficient crack segmentation method [4], two simple statistical features are computed: (i) the standardization of pixel intensities (z-score) belonging to the set of crack seeds; (ii) the z-score of non-crack pixel intensities. An iterative procedure is then followed, that can relabel some of the originally non-crack pixels as additional crack pixels, if they can be modelled by the corresponding distribution and are neighbors of existing crack pixels. The algorithm iterates, updating the z-score distributions, until the automatically determined stopping criteria, detailed in Section II, is met.

The proposed crack detection system initially pre-processes the images, testing three different smoothing algorithms, and then performs crack segmentation. Finally cracks are classified according to their orientation as either longitudinal, transversal or miscellaneous [5].

The paper is organized as follows: section II describes the proposed crack segmentation algorithm, able to identify cracks with complex shapes, section III presents experimental results for road flexible pavement images acquired with different types of sensors, and section IV concludes the paper and presents hints for future work.

## II. SYSTEM ARCHITECTURE

The architecture of the proposed crack segmentation algorithm is presented in Figure 1. When dealing with road images it is important to reduce the intensity variance of pixels belonging to the healthy pavement areas (image background), without affecting the intensity of those pixels affected by cracks – this is the goal of the pre-processing stage. The next stage is the identification of a set of crack segments (the “crack seeds”), trying to minimize the inclusion of false positives. Then, the novel crack segmentation refinement is presented, to obtain an improved identification of cracks, even when they present multiple branches. Finally, a type classification can be assigned to each identified crack.

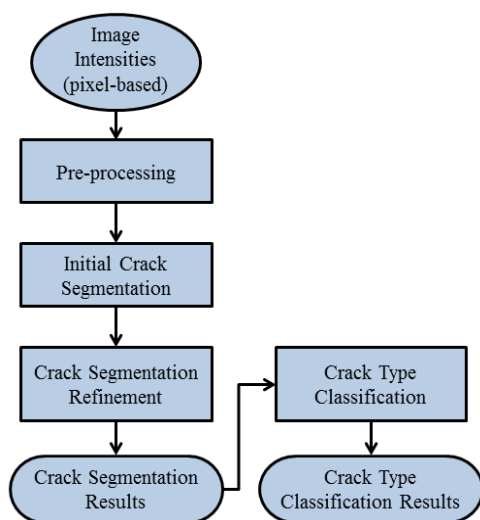


Fig. 1. Architecture of proposed crack segmentation algorithm.

### A. Pre-processing

This paper confronts three different pavement surface image pre-processing strategies: (i) anisotropic diffusion; (ii) wavelet denoising; (iii) morphological filtering. Each of these is briefly discussed in the following, all of them aiming to smooth the input images and enable a better crack segmentation performance.

Pre-processing using anisotropic diffusion follows the algorithm of Perona and Malik [6]. The variables to be set for this algorithm are: (i) number of iterations,  $it$ ; (ii) conduction coefficient,  $cc$ , where for low values of  $cc$  small intensity gradients are able to block conduction and hence diffusion across step edges, while higher  $cc$  values reduce the influence of intensity gradients on conduction; (iii) diffusion speed,  $\lambda$ , a constant taking values in the range 0 to 0.25, as suggested in [6]. Experimentation was conducted on road pavement surface images, varying  $it$  from 1 to 12 and  $cc$  from 20 to 100, with step 10, for the maximum diffusion speed ( $\lambda = 0.25$ ) since the objective is to efficiently reduce the variance of pixel

intensities. The best results, in view of the subsequent crack segmentation stages, were obtained with an anisotropic diffusion model that favors wide regions, using  $it = 4$  and  $cc = 60$ . These results show a considerable pixel intensity variance reduction, without significantly deteriorating the crack information, as reported in [4].

Pre-processing with the stationary wavelet transform uses the *Symlet* decomposition filters (SWT). This technique aims to reduce the unwanted random texture found in non-crack regions, while trying to keep the regions with cracks well defined. The implementation proposed in [7] is adopted, using a fourth order *Symlet* decomposition filter, with four level decomposition and hard thresholding, empirically adjusted after exhaustive testing, to achieve a good compromise between smoothing and computational time.

The third pre-processing strategy applies a combination of the morphological *erosion* and *opening* operations [8], according to equation (1):

$$I_{Smoothed} = I_{Eroded} \odot se = (I \ominus se) \odot se = [(I \ominus se) \ominus se] \oplus se \quad (1)$$

where  $I$  is the original image,  $\odot$  represents the morphological *opening* operator, the symbols  $\ominus$  and  $\oplus$  stand for the *erosion* and *dilation* operators, respectively. For road pavement surface images, this morphological filtering reduces pixel intensity variance in non-crack areas, while making crack regions appear more pronounced since its application results in a thickening of darker image regions.

Results of applying the three pre-processing strategies to two sample images are included in Figure 2. It can be observed that all pre-processing strategies are able to significantly reduce pixel intensity variance, without deteriorating the crack information. The intensity difference between crack and non-crack pixels is increased, and consequently the same happens to the separability of the two classes considered, thus easing the subsequent segmentation and reducing the number of false positive detections. These results seem to slightly favor the wavelet pre-processing, as it better maintains the original average intensity values and maximizes the crack pixel separation. Nevertheless, even the simpler morphological filtering, with a disk-shape structuring element of 3 pixel radius, is able to provide desired smoothing results, to be considered as input to a segmentation algorithm.

### B. Initial Crack Segmentation

The goal of the second stage of the proposed system is to identify a set of crack seeds. This initial crack segmentation is obtained by thresholding the histogram of smoothed image intensities, according to the algorithm presented in [4]. This algorithm fits a Gaussian function to the histogram and selects the segmentation threshold as the intensity value presenting a statistical significance level of 5% ( $I_{th0.05}$ ), i.e, the threshold value will be  $\mu - 1.96 \times \sigma$ , where  $\mu$  and  $\sigma$  are, respectively, the mean and standard deviation parameters of the Gaussian.

For the proposed system false positives are to be avoided at this stage, so the selected crack seeds should additionally respect two rules: (i) the width of each connected component ( $cc$ ) should be equal to or greater than  $w$ ; (ii) the length of the

ellipse's major axis, fitted to each cc, should be greater than  $lg$ . To choose values for these parameters, the 44 pavement surface images without cracks, available from both image datasets tested (see details in Section III), are considered, to understand the distribution of the false positive cracks detected. The histograms for the  $w$  and  $lg$  parameters observed in the false positive cracks are shown in Figure 3. The rule parameter values selected are:  $w = 2$  mm, for cc width, and  $lg = 25$  mm, for the ellipse's major axis length.

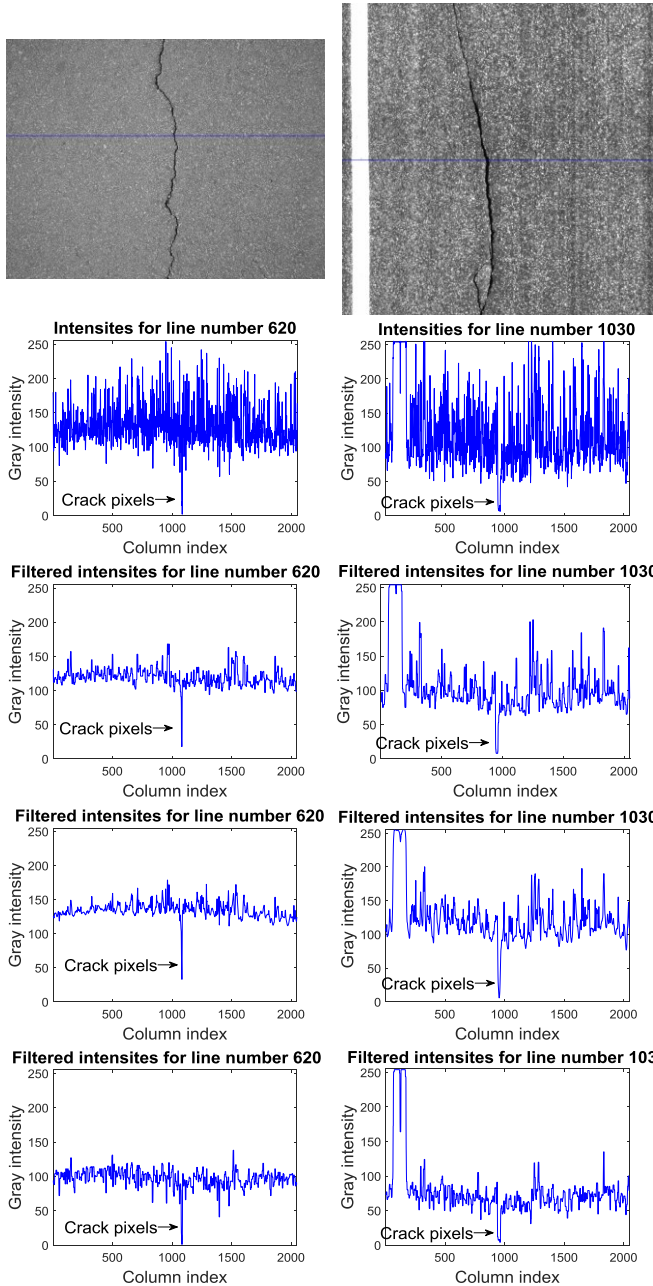


Fig. 2. Sample pre-processing results: sample images (top row); original intensities (2<sup>nd</sup> row); anisotropic diffusion (3<sup>rd</sup> row); wavelet denoising (4<sup>th</sup> row); morphological filtering (bottom row).

### C. Crack Segmentation Refinement

The novel crack segmentation refinement algorithm takes as input the set of initial crack seeds, which is expected not to

contain many connected components falsely labeled as cracks. Its architecture is shown in Fig. 4. The goal is to link together narrow and short crack sections that may have been identified as separate connected components. For this, the crack seeds are extended by relabeling non-crack pixels, in the vicinity of crack connected components, which share the same statistical properties as those already known to belong to the cracks class.

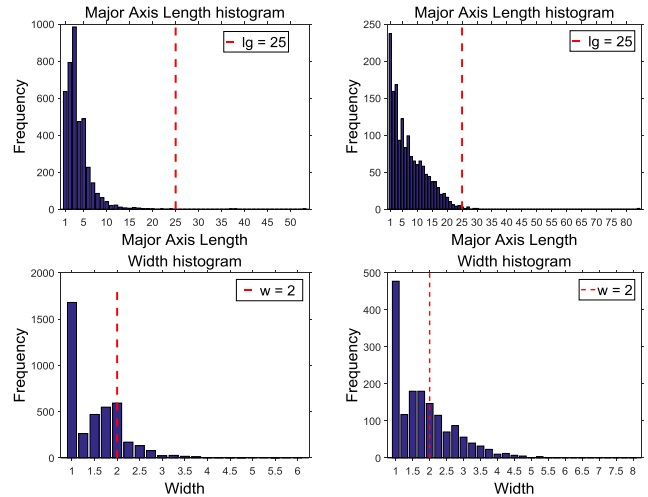


Fig. 3. Histograms of widths ( $w$  in mm) and lengths ( $lg$  in mm) of connected components of the initial segmentation found in both image databases: ImgSet1 (left), ImgSet2 (right).

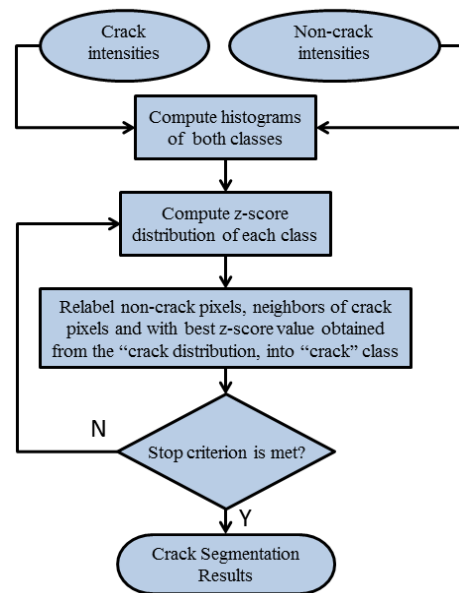


Fig. 4. Crack segmentation refinement algorithm.

The segmentation refinement starts by the computation of the two z-score histograms, for the normalized intensity values of pixels from the crack and the non-crack classes. An iterative procedure is then followed, relabeling some of the originally non-crack pixels as additional crack pixels if they can be modelled by the corresponding distribution. All non-crack pixels with intensities presenting a statistical significance lower than 5% when considering the z-score for the non-crack class, and simultaneously a statistical significance higher than 5%

when considering the crack class z-score, and at the same time are neighbors of an existing crack seed, have their class labels changed to “crack”. The procedure is iterated, computing new histograms for the updated crack and non-crack classes.

The iterative process stops when the rate of pixels classified as crack ( $R_c$ ), before and after each iteration, defined in equation (2), exceeds an empirically set threshold of 5%:

$$R_c = (N_i - N_{i-1}) / N_{i-1} \quad (2)$$

where  $N_i$  and  $N_{i-1}$  are the number of crack pixels after the present and the previous iterations, respectively.

Segmentation results for a sample image detail are included in Figure 5, showing an initial set of three crack segments (left), which were aggregated into a single crack segment, by the proposed crack segmentation refinement algorithm (right).

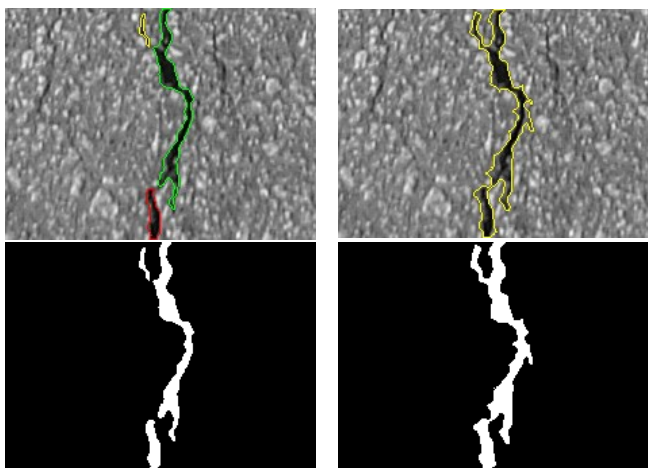


Fig. 5. Sample crack segmentation results: initial crack seeds (left) and after crack segmentation refinement (right).

### III. EXPERIMENTAL RESULTS

To evaluate the performance of the proposed crack segmentation algorithm, two different datasets were considered. The first, *ImgSet1*, is a dataset acquired with a photographic camera during a visual pavement surface survey of a Portuguese road, including 56 gray level images of size  $1536 \times 2048$  pixels, which is publicly available at <http://amalia.img.lx.it.pt/CrackIT/>. This dataset includes 8 images without any type of road pavement surface distress. The second dataset, *ImgSet2*, was acquired by the laser road imaging system LRIS [9], during a survey of a Canadian road, including 166 images of size  $4096 \times 2048$ . This dataset includes 36 images not containing cracks. For both datasets the images were acquired with each pixel corresponding to approximately  $1 \text{ mm}^2$  of the road pavement.

To overcome the difficulties in creating a pixel-based segmentation ground-truth (maybe not an achievable task), a block-based ground truth data was considered, where a human expert manually labelled  $75 \times 75$  pixel image blocks with cracks, by selecting them over the original road pavement surface image. A quantitative evaluation of crack segmentation results can be computed using this information. Additionally, a qualitative evaluation is also considered, by evaluating the crack type classification results, using the approach developed in [5], which takes as input the crack segmentation results.

The proposed crack segmentation algorithm was implemented using Matlab 2016b, set up for parallel processing with a pool of 4 workers, using a Toshiba Qosmio X-70-B-10T with an Intel Core i7-4720 HQ CPU and 16Gb of RAM, with pre-installed Windows 10 operating system.

Figure 6 presents sample crack segmentation results, for details containing cracks of three images selected from both datasets (see top row). Tests consider the three preprocessing strategies: (i) anisotropic diffusion favoring wide regions, with  $it = 4$  and  $cc = 60$  (see 2<sup>nd</sup> and 3<sup>rd</sup> rows); (ii) stationary wavelet transform with fourth order *Symlet* decomposition filters (see 4<sup>th</sup> and 5<sup>th</sup> rows); (iii) morphological filtering with a 3 pixel radius disk-shaped structuring element (see 6<sup>th</sup> and 7<sup>th</sup> rows).

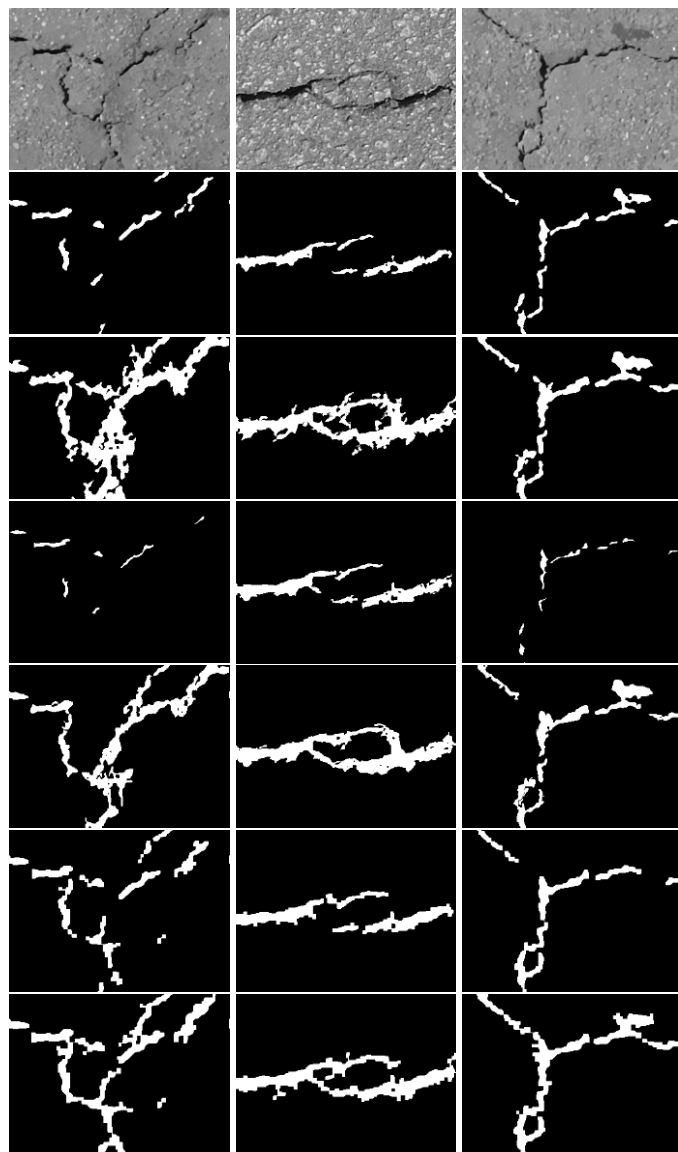


Fig. 6. Sample crack segmentation results. Each pair of rows shows the crack seeds (upper row) and the crack segmentation refinement (lower row). Results for the three processing techniques are included: anisotropic diffusion (top), wavelet transform (middle) and morphological filtering (bottom).

Looking into the results presented in Figure 6, the binary images corresponding to each pre-processing strategy include

the crack seeds (upper row) and the crack segmentation refinement result (lower row). When using the anisotropic diffusion pre-processing, the initial 10, 9, and 10 connected components (crack seeds), were merged among themselves to result in 4, 6, and 7 connected components, after 6, 6 and 4 iterations, respectively for the left, middle and right columns. When considering the stationary wavelet transform pre-processing, the initial number of crack seed connected components were 4, 9 and 11, being reduced to 4, 7 and 6 crack segments, after a number of 4, 4, and 5 iterations, respectively. Results for the morphological filtering pre-processing strategy show an initial number of 12, 7 and 5 crack seed connected components, reduced to 5, 6 and 3 crack segments, after a number of 6, 7 and 3 iterations, respectively.

A visual analysis of the obtained results allows concluding that images processed using the anisotropic diffusion originates thicker connected components in comparison to the other two pre-processing techniques, resulting in a lower number of crack seed connected components. The stationary wavelet transform tends to originate larger gaps between crack seed components, while the morphological filtering pre-processing seems to perform well, not thickening too much the crack seed segments. The results after applying the proposed crack segmentation refinement show that many of the gaps existing between the crack seeds are properly filled.

The quantitative results achieved using the block-based ground truth, based on the *recall* metric (ratio between the number of blocks correctly classified as cracks and the total number of ground truth crack blocks) was: 88.2%, 90.2%, and 94.3% for *ImgSet1*; and 85.3%, 91.3, 93.4% for *ImgSet2*, in relation to the anisotropic diffusion, wavelet and morphological smoothing techniques, respectively. Analyzing the results for all images of both image datasets, the number of iterations ranged from 2 to 12, while the computational time ranged from 11 to 23 seconds for the entire processing of each image.

TABLE I. CRACK TYPE CHARACTERIZATION RESULTS USING THE PROPOSED MORPHOLOGICAL PRE-PROCESSING.

Dataset	Classification type	Crack Types		
		Long.	Transv.	Misc.
ImgSet1	Ground Truth	50	5	17
	Manually labelled and detected by the system	50	5	17
	Not manually labelled but detected by the system	4	2	3
ImgSet2	Ground Truth	125	12	43
	Manually labelled and detected by the system	125	12	43
	Not manually labelled but detected by the system	11	2	6

Although quantitative results are similar to those published in [4], the proposed segmentation was able to include small regions labelled as cracks in the neighborhood of ground truth crack blocks, which were not manually labelled as crack blocks since the number of crack pixels they included was low. Notice that all cracks manually labeled as cracks were correctly labeled by the proposed strategy, as can be seen in Table I, corresponding to a 100% recall. The blocks not

manually labeled by the human expert as containing cracks, but detected by the proposed system, were visually confirmed to contain short and thin crack segments added by the improved segmentation algorithm proposed. They correspond to additional pavement surface areas in the images that should be kept under observation when performing further road pavement surface inspections or planning maintenance and repair actions.

#### IV. CONCLUSIONS AND FUTURE WORK

This paper proposed a novel crack segmentation refinement algorithm, which is able to follow complex cracks including several thin branches or presenting a long linear development. The system performs well with the three different pre-processing strategies tested, eventually favoring the simple morphological filtering. Both quantitative and qualitative performance evaluations indicate improved segmentation results.

Future work includes: (i) testing the proposed algorithm in images with cracks tangled by shadows; (ii) consider an alternative automatic stop criterion, by analyzing the evolution of the derivative of the rate of pixels classified as cracks ( $R_c$ ); (iii) exploitation of Compute Unified Device Architecture (CUDA) based GPUs, to reduce the processing time.

#### ACKNOWLEDGMENT

The authors acknowledge the support of Fundação para a Ciência e Tecnologia (FCT) and Instituto de Telecomunicações (<http://www.it.pt/>), under Project UID/EEA/50008/2013.

#### REFERENCES

- [1] AASHTO, "Standard Specifications for Transportation Materials and Methods of Sampling and Testing, and AASHTO Provisional Standards", Washington, USA: American Association of State Highway and Transportation Officials, 2016.
- [2] Comité technique 4.2 Interaction route/véhicule / Technical Committee 4.2 Road/Vehicle Interaction, "Evaluating the performance of automated pavement cracking measurement equipment", World Road Association, <https://www.piarc.org/>, 2008.
- [3] Rabih Amhaz, Sylvie Chambon, Jérôme Idier, Vincent Baltazart, "Automatic Crack Detection on Two-Dimensional Pavement Images: An Algorithm Based on Minimal Path Selection", IEEE Transactions on Intelligent Transportation Systems, vol. 17, no. 10, pp. 2718-2729, October 2016.
- [4] H. Oliveira and P. Correia, "Automatic Crack Detection on Road Imagery Using Anisotropic Diffusion and Region Linkage", EUSIPCO 2010, Alborg, Denmark, August 23-27, 2010.
- [5] H. Oliveira and P. Correia, "CrackIT – An image processing toolbox for crack detection and characterization", IEEE International Conf. on Image Processing - ICIP, Paris, France, October 27-30, 2014.
- [6] P. Perona and J. Malik, "Scale-space and Edge Detection Using Anisotropic Diffusion", IEEE Transactions on Pattern Analysis and Machine Intelligence, vol. 12, no. 7, pp. 629-639, July 1990.
- [7] M. Misiti, Y. Misiti, G. Oppenheim e J. Poggi, "Wavelet Toolbox™ 4 User's Guide", Matlab, Ed., MatWorks, 2016.
- [8] R. Gonzalez, R. Woods and S. Eddins, "Digital Image Processing Using Matlab, New Jersey: Pearson Prentice Hall, 2004.
- [9] LRIS, "Pavementrics: Laser Road Imaging System (LRIS)," 2013. [Online]. Available: <http://www.pavementrics.com/applications/road-inspection/laser-road-imaging-system/> [Accessed on 25 January 2017].